New Journal of Physics
The open-access journal for physics

Characterization of the second-harmonic response of a silver–air interface

K A O'Donnell[1] **and R Torre**[2,3]

[1] División de Física Aplicada, Centro de Investigación Científica y de Educación Superior de Ensenada, Apartado Postal 2732, Ensenada, Baja California, 22800 México
[2] Dipartimento di Fisica and European Laboratory for Non-linear Spectroscopy (LENS), Polo Scientifico, Università di Firenze, Via Carrara n.1, Sesto Fiorentino, 50019, Italy
[3] INFM CRS-SOFT, Università La Sapienza, Roma, Italy
E-mail: odonnell@cicese.mx

New Journal of Physics **7** (2005) 154
Received 11 May 2005
Published 5 July 2005
Online at http://www.njp.org/
doi:10.1088/1367-2630/7/1/154

Abstract. We present an experimental study of second-harmonic generation in the light reflected from a flat silver surface. It is discussed that the harmonic generation from such a surface may be expressed in terms of the three unique elements of its effective surface susceptibility tensor. A method is proposed to determine the susceptibilities by measuring the second-harmonic power with different polarization conditions. By employing a picosecond light source and photon-counting techniques, we determine the susceptibilities and compare our results with previous work.

Contents

PII: S1367-2630(05)99707-3

1. Introduction

Over the years, there have been many studies of second-harmonic generation in the light specularly reflected from the flat surface of an evaporated metal. In early works, the effects were observed experimentally and efforts were directed towards understanding the physical mechanisms responsible [1]–[3]. Later works have developed more sophisticated models of the surface nonlinearities [4]–[16], and experimental results have improved considerably as better laser sources have been developed [17]–[19]. Other research has expanded the field to include applications as an analytical tool in surface science [20], or in studies of roughened metals where the consequences of surface wave excitation or multiple scattering can dominate the harmonic generation [21].

Of course, the bulk of an isotropic metal has inversion symmetry so that the electric dipole part of its nonlinear susceptibility must vanish. The harmonic generation is thus weak and has other origins. In particular, the nonlinearity receives contributions from both the surface as well as the bulk of the metal [22]. The bulk contribution is due to higher-order terms in the body of the metal, while the surface contribution arises from the steep electric field gradient as well as the abrupt change in material properties at the surface. By integrating the surface terms across the interface layer (of thickness of perhaps a few tenths of nanometres), and adding in the net bulk contribution (occurring within a few skin depths of the surface), one may obtain the total nonlinear response.

For reflection from an isotropic metal, the inherent symmetries guarantee that there are only three distinct elements of the surface susceptibility tensor [23]. A clear goal would seem to be their determination but, in experimental work, there have been few such studies. A common measurement is the harmonic signal for p incident and detected polarization [17, 18] that provides the strongest signal but, as will be described later, depends in a complicated way on all three susceptibilities. Some early works [1]–[3] have measured the second-harmonic power for different polarization conditions from which, at least, some susceptibilities or ratios of susceptibilities can be determined. This was an encouraging development, but it has been pointed out that conclusions drawn in early work may be questionable due to angular factors missing in the then-existing theories ([15], see p 21). Quite recently, some detailed measurements of the susceptibilities have been reported [19] that we will discuss in more detail later. Also, there has been renewed interest in the three tensor elements because they are essential to the understanding of second-harmonic generation from randomly rough metals, where a number of interesting effects have appeared in recent years [21]. However, the values of the susceptibilities are still open to debate and comparisons of theory and experiment for rough surfaces have thus remained, at best, significantly ambiguous.

Here, we thus present an example of fully characterizing the harmonic response through experimental determination of the three unique susceptibilities of a metal surface. Firstly, we present an expression for the second-harmonic power for arbitrary incident and detected polarization conditions and, from it, we discuss the procedure for determining the susceptibilities. For the case of an evaporated silver surface, the susceptibilities are determined from a series of measurements with different polarization conditions. Some results are at signal levels well-below those of the p-polarized case, but they are readily measurable with sensitive detectors and modern laser sources. We measure the dependence of all quantities on angle of incidence, which allows us to test for consistency with the angular-dependence of the theoretical expressions. Our results

are compared with the predictions of theoretical calculations and, as possible, with previous experimental results.

A few general comments are appropriate at this point. Firstly, the experimental technique has wider applicability and is appropriate for surfaces of other isotropic media, as well as for two crystal symmetry classes having the same three unique susceptibilities [23]. A second point is that the nomenclature employed in this field varies widely; in the next section we therefore make efforts to relate our formulation of the problem to works employing other notational schemes. A final point concerns the spirit in which our experimental results are to be taken. In particular, it is undoubtedly true that the harmonic response of a metal is strongly dependent on surface preparation. Thus it is not realistic to claim that our experimental results could have completely general validity. Instead it is only claimed that, for a sample prepared under our typical conditions, the results presented here represent typical values. Indeed, it would be better to repeat the procedures outlined here with any sample of particular interest.

2. Theoretical considerations

For arbitrary incident and detected polarization conditions, the reflected second-harmonic power $P(2\omega)$ may be written as

$$P(2\omega) = \frac{32\pi^3\omega^2}{c^3(\pi w^2)} P^2(\omega)\tan^2(\theta)|\beta_{pp}\cos^2(\gamma)\cos(\gamma')\exp(\mathrm{i}[2\delta+\delta']) + \beta_{sp}\sin^2(\gamma)\cos(\gamma')\exp(\mathrm{i}\delta') + \beta_{+s}\sin(2\gamma)\sin(\gamma')\exp(\mathrm{i}\delta)|^2, \quad (1)$$

where $P(\omega)$ is the power incident at fundamental frequency ω, θ is the angle of incidence, and w is the e^{-1} amplitude radius of the illuminating beam. The angle γ and the phase angle δ specify the incident polarization state; the projections of this normalized state on to the directions of p and s polarization are, respectively, $\mathrm{e}^{\mathrm{i}\delta}\cos\gamma$ and $\sin\gamma$, with time dependence $\mathrm{e}^{-\mathrm{i}\omega t}$ suppressed. Similarly, the output state at 2ω has been projected on to the unit state $(\mathrm{e}^{\mathrm{i}\delta'}\cos\gamma', \sin\gamma')$ in its (p, s) polarization directions. The β's of equation (1) are related to the effective surface susceptibility tensor elements χ_{ijk} through

$$\beta_{pp} = t_p^2(\omega)t_p(2\omega)\sqrt{\epsilon(2\omega)}\left\{\frac{\sin^2(\theta)}{\epsilon(\omega)}[\epsilon^2(\omega)\chi_{\perp\perp\perp} - \chi_{\perp\parallel\parallel}] + \chi_{\perp\parallel\parallel} - 2\frac{\sqrt{\epsilon(\omega)-\sin^2(\theta)}\sqrt{\epsilon(2\omega)-\sin^2(\theta)}}{\epsilon(2\omega)}\chi_{\parallel\parallel\perp}\right\}, \quad (2)$$

$$\beta_{sp} = t_s^2(\omega)t_p(2\omega)\sqrt{\epsilon(2\omega)}\chi_{\perp\parallel\parallel}, \quad (3)$$

and

$$\beta_{+s} = t_p(\omega)t_s(\omega)t_s(2\omega)\sqrt{\epsilon(\omega)}\chi_{\parallel\parallel\perp}, \quad (4)$$

where $t_p(\Omega)$ and $t_s(\Omega)$ are Fresnel transmission coefficients as in

$$t_p(\Omega) = \frac{2\sqrt{\epsilon(\Omega)}\cos\theta}{\epsilon(\Omega)\cos\theta + \sqrt{\epsilon(\Omega)-\sin^2(\theta)}}, \quad (5)$$

and

$$t_s(\Omega) = \frac{2\cos\theta}{\cos\theta + \sqrt{\epsilon(\Omega) - \sin^2(\theta)}}, \tag{6}$$

with $\epsilon(\Omega)$ being the metal's complex dielectric constant at frequency Ω. We have developed equations (1)–(4) from the formalism of [16]. However, in the result given in [16] (their equation (4.13)), the term involving $\chi_{\parallel\parallel\perp}$ in β_{pp} is missing, and there are several typographical errors that have been corrected in equations (1)–(4). On the other hand, equations (1)–(4) are fully consistent with the p and s second-harmonic amplitudes in the thesis of Heinz [15].

We have chosen a coordinate system in which the metal surface is the $x - y$ plane and the $+z$-axis extends into the metal. The three unique, nonvanishing susceptibility tensor elements in equations (2)–(4) are then $\chi_{\perp\perp\perp} = \chi_{zzz}$, $\chi_{\perp\parallel\parallel} = \chi_{zxx} = \chi_{zyy}$ and $\chi_{\parallel\parallel\perp} = \chi_{xxz} = \chi_{xzx} = \chi_{yyz} = \chi_{yzy}$, with the equalities being obvious from symmetry. The particular conventions for χ_{ijk} vary in the literature. We have chosen to consider χ_{ijk} as relating the nonlinear polarization to the fundamental electric fields in a plane just above the metal or, equivalently, to the **F**-field defined elsewhere [22, 23]. The χ_{ijk} of Heinz [15] (H) or of Mizrahi and Sipe [16] (MS) are then related to those of equations (2)–(4) through

$$\chi_{\perp\perp\perp} = \frac{1}{\epsilon'^2(\omega)\epsilon'(2\omega)}\chi^{(H)}_{\perp\perp\perp} = \frac{1}{\epsilon^2(\omega)}\chi^{(MS)}_{\perp\perp\perp}, \tag{7}$$

$$\chi_{\perp\parallel\parallel} = \frac{1}{\epsilon'(2\omega)}\,\chi^{(H)}_{\perp\parallel\parallel} = \chi^{(MS)}_{\perp\parallel\parallel} \tag{8}$$

and

$$\chi_{\parallel\parallel\perp} = \frac{1}{\epsilon'(\omega)}\chi^{(H)}_{\parallel\parallel\perp} = \frac{1}{\epsilon(\omega)}\chi^{(MS)}_{\parallel\parallel\perp} \tag{9}$$

These differences arise because Mizrahi and Sipe use electric fields evaluated in the metal to define $\chi^{(MS)}_{ijk}$, while Heinz considers the metal to have a vanishingly thin nonlinear overlayer with the primed dielectric constants, with $\chi^{(H)}_{ijk}$ relating the polarization and electric field within the layer.

On the other hand, it is stressed that $P(2\omega)$ of equation (1) is a fundamental result in the sense that the form of its dependence on the three distinct χ_{ijk} is a consequence solely of symmetry; it does not depend on the particular conventions or models employed. Results from other works may be obtained by transforming equation (1) according to the choice of conventions used (e.g., as in equations (7)–(9)). This general nature of equation (1) also makes clear the essential task at hand: to develop means of calculating the three unique χ_{ijk} from whatever theoretical approach is employed or, in experimental work, to devise a means of measuring them.

All χ_{ijk} of equations (2)–(4) contain contributions from both the surface and bulk of the metal. Specifically,

$$\chi_{\perp\perp\perp} = \chi_{s,\perp\perp\perp} - \frac{(\gamma_b + \chi^Q_1)}{\epsilon^2(\omega)\epsilon(2\omega)}, \tag{10}$$

$$\chi_{\perp\parallel\parallel} = \chi_{s,\perp\parallel\parallel} - \frac{(\gamma_b + \chi^Q_2)}{\epsilon(2\omega)} \tag{11}$$

and

$$\chi_{\parallel\parallel\perp} = \chi_{s,\parallel\parallel\perp} - \frac{\chi_4^Q}{\epsilon(\omega)}, \tag{12}$$

where χ_s denotes the true surface part, γ_b is the usual bulk contribution and the χ_i^Q represent elements of the bulk electric quadrupole susceptibility. The bulk parameter γ_b has been known for many years (and indeed γ_b was included explicitly in the results of [16], although here we consider it an integral part of the total χ_{ijk} as in equations (10)–(11)), but the other χ_i^Q bulk contributions were first pointed out in [22]. Because all susceptibilities include both surface and bulk contributions, the isolation of a pure surface effect is not easily possible, and all results to be presented here are thus for the total χ_{ijk}.

To compare with other formulations, we note that early works [1]–[3] employed three nonlinear parameters that are related to the three χ_{ijk}. Also, there is another common notation in which the χ_{ijk} are replaced by three dimensionless parameters $a(\omega)$, $b(\omega)$ and $d(\omega)$. This convention dates back to the free-electron model of Rudnick and Stern [4] and has been widely used in later works [5]–[14]. As far as the surface nonlinear constants are concerned, it may be considered a simplification of the general case. In this model, it is assumed that $\chi_{s,\perp\parallel\parallel} = 0$ and that $\chi_i^Q = 0$ in equations (10)–(12). One then characterizes the nonlinearity through the three remaining free parameters of equations (10)–(12) as

$$a(\omega) = \frac{16\pi m\omega^2}{e}\frac{\epsilon^2(\omega)}{\epsilon(\omega)-1}\chi_{s,\perp\perp\perp}, \tag{13}$$

$$b(\omega) = \frac{16\pi m\omega^2}{e}\frac{\epsilon(\omega)}{\epsilon(\omega)-1}\chi_{s,\parallel\parallel\perp}, \tag{14}$$

and

$$d(\omega) = -\frac{32\pi m\omega^2}{e}\frac{1}{\epsilon(\omega)-1}\gamma_b, \tag{15}$$

where m and e are the electron mass and charge, and where a Drude model for $\epsilon(\omega)$ has been assumed.

In closing, it may be noted that γ_b sometimes appears elsewhere with a different sign [16]. The sign difference is a consequence of assuming the $+z$-axis to be directed into the free space above the metal, which inverts the relative sign of γ_b with respect to the χ's. Also, $\chi_{\parallel\parallel\perp}$ sometimes appears with a value twice that used here [13]. This situation arises because we sum all (i.e., even non-unique) terms arising in the tensor product in the calculation of $P(2\omega)$, while [13] does not count redundant terms.

3. Experimental results

We now present our method of experimentally determining $\chi_{\perp\perp\perp}$, $\chi_{\perp\parallel\parallel}$ and $\chi_{\parallel\parallel\perp}$ from the polarization-dependence of $P(2\omega)$. The approach follows from the interpretation of equations

(1)–(4). The term β_{pp} of equation (2) represents the conversion of p-polarized ω light to p-polarized 2ω light, as is clear from its factors $\cos^2(\gamma)$ and $\cos(\gamma')$ in equation (1). Similarly, from the associated angular factors in equation (1), β_{sp} represents the transformation of s incident to p reflected light, while β_{+s} predicts the emission of s-polarized 2ω light under illumination by a mixed ω polarization state, which occurs optimally for $\gamma = 45^\circ$.

These considerations suggest the method of determination of $\chi_{\perp\perp\perp}$, $\chi_{\perp\parallel\parallel}$ and $\chi_{\parallel\parallel\perp}$. In particular, a measurement of $P(2\omega)$ with $(\gamma, \gamma') = (90^\circ, 0^\circ)$ isolates the β_{sp} term in equation (1), determining $\chi_{\perp\parallel\parallel}$. A second measurement of $P(2\omega)$ with $(\gamma, \gamma') = (45^\circ, 90^\circ)$ isolates the β_{+s} term and determines $\chi_{\parallel\parallel\perp}$. Finally, a third measurement of $P(2\omega)$ with $(\gamma, \gamma') = (0^\circ, 0^\circ)$ isolates the term in β_{pp} which, as is clear from equation (2), depends on all three χ_{ijk}. However, since $\chi_{\perp\parallel\parallel}$ and $\chi_{\parallel\parallel\perp}$ are known at this point, $\chi_{\perp\perp\perp}$ may be determined with some care. In what follows, we provide a study of the complete θ-dependence of these three data sets, which improves the accuracy of the measured χ_{ijk} and allows comparison of data with the predicted angular forms.

The metal surface was prepared on a glass substrate in a filament evaporator using standard vacuum deposition techniques. A thick layer (400 nm) of 0.9999 pure silver was deposited at a rate of approximately 1 nm s^{-1}, while vacuum chamber pressure was kept well below 10^{-6} Torr. The sample was kept in a nitrogen atmosphere until it was mounted in the optical experiment. There, pulses from a mode-locked Coherent Antares Nd : YAG laser were sent to a Spectra Physics 3800RA injection-seeded regenerative amplifier. The output pulses obtained were of wavelength $\lambda = 1064$ nm, FWHM 100 ps, peak power 10 MW and repetition rate 1 kHz. The slightly convergent incident beam had a width $w = 2.0$ mm at the sample. A photon-counting photomultiplier (mounted on a 60 cm arm) and the sample were mounted on different concentric motorized rotation stages to vary θ. A Stanford Research SR400 photon counter was gated to accept photocounts within a 5 ns window coinciding with each laser pulse and photocounts were averaged for 10 seconds to obtain each data point.

An infrared filter was placed in the incident beam to remove any inadvertent 2ω light, while the detector was preceded by a $CuSO_4$/water solution cell, a Schott BG39 glass filter and a 532 nm wavelength interference filter to isolate 2ω light. Firing full laser power directly into the detector produced a signal of less than 1 photon s^{-1}. No metal surface damage or surface plasma was ever observed during the experiments, which is a consequence of the low 1 mJ pulse energy. In the data taken in reflection from the metal, it was verified that the photocount rate rose as the square of the incident fundamental power, but was linearly dependent on the generated 2ω power. In a final step, all data were normalized through comparison with additional measurements of Maker fringes [24] in second-harmonic generation from a window of crystalline quartz, for which the nonlinear constants are well-established. We thus present data in the normalized form $R(2\omega)$ given by

$$R(2\omega) \equiv \frac{P(2\omega)}{P^2(\omega)/(\pi w^2)}, \tag{16}$$

so as to remove the incident beam power- and area-dependence from equation (1).

Figure 1(A) presents measurements of $R(2\omega)$ with $(\gamma, \gamma') = (90^\circ, 0^\circ)$ (i.e., s to p polarization conversion). The photon rates are at most 18 $second^{-1}$, but a curve clearly rises above noise levels. A least-squares fit to $R(2\omega)$ is also shown and determines $\chi_{\perp\parallel\parallel}$ as 1.22×10^{-14} cm^2 $statvolt^{-1}$ or 5.11×10^{-16} cm^2 V^{-1} where we have chosen, somewhat arbitrarily, the sign of $\chi_{\perp\parallel\parallel}$ as positive. To support the validity of these data even at such low levels, a second measurement of $R(2\omega)$ is

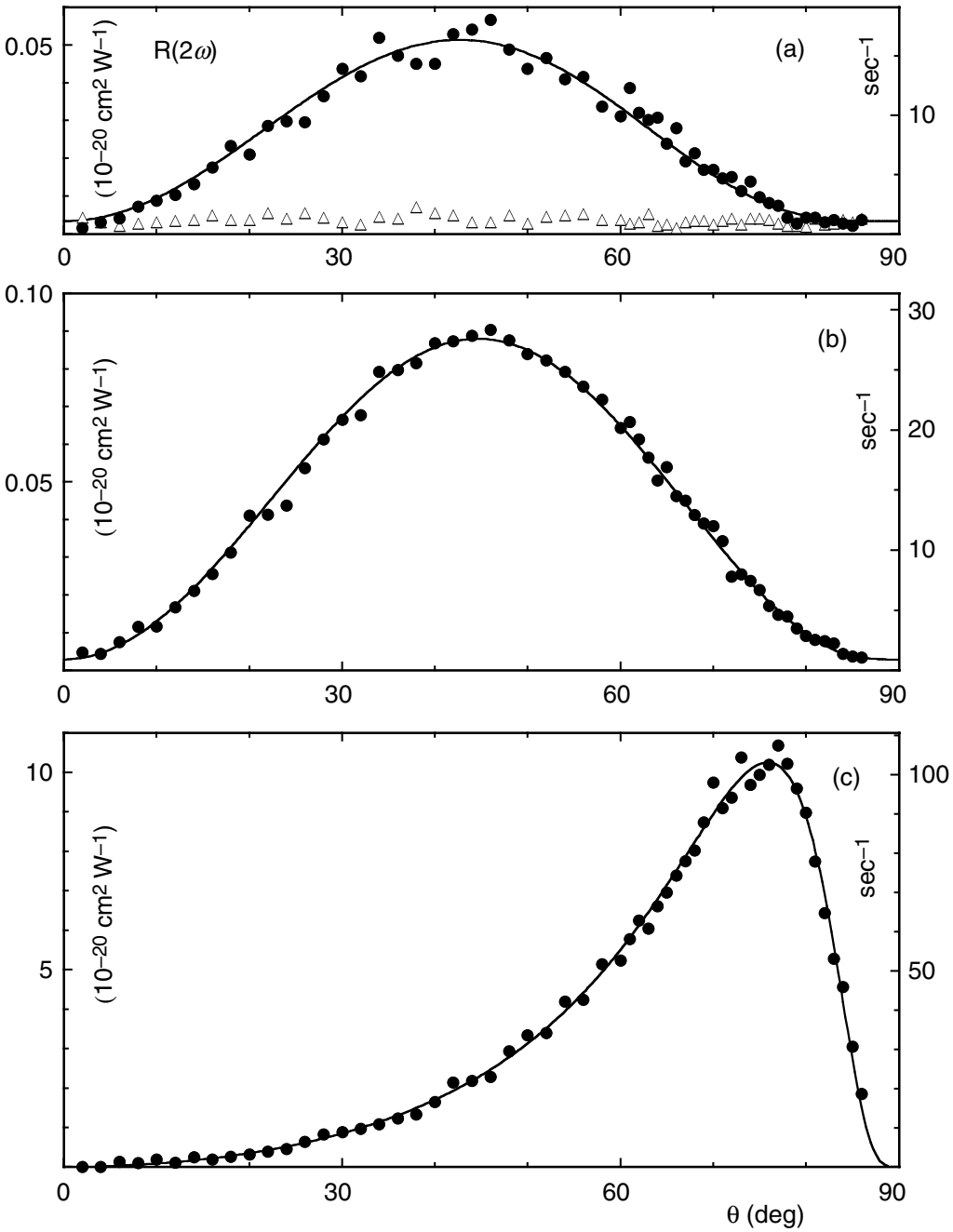

Figure 1. Measured second-harmonic power (●) as a function of incident angle θ compared with fits to equation (1) (——). Vertical axes denote conventional normalization (left) and photon rate (right). Cases shown are: (a) s incident and p detected polarization, (b) 45° incident and s detected polarization and (c) p incident and p detected polarization. The triangles in (a) are data for s incident and s detected polarization which is forbidden by symmetry; the fits in (a) and (b) include a constant background count rate of approximately 1 second^{-1}.

also included in figure 1(A) for $(\gamma, \gamma') = (90^\circ, 90^\circ)$, which is predicted to be zero by equation (1). This measurement has residual signal levels of only 1–2 second^{-1}, so that the previous result appears to be significantly above possible background levels.

Figure 1(B) presents results for the emission of s-polarized 2ω light with $(\gamma, \gamma') = (45^\circ, 90^\circ)$. The signal is somewhat stronger and reaches a peak of 28 second^{-1}. The least-squares fit to $R(2\omega)$ is again good and determines $\chi_{\parallel\parallel\perp}$ as -6.00×10^{-15} cm^2 statvolt^{-1} or -2.52×10^{-16} cm^2 V^{-1}. Even though $R(2\omega)$ is here proportional to $|\chi_{\parallel\parallel\perp}|^2$, we have given $\chi_{\parallel\parallel\perp}$ a negative sign for reasons that will soon be apparent.

The third measurement for p incident and p detected polarization with $(\gamma, \gamma') = (0^\circ, 0^\circ)$ is shown in figure 1(C). Here, there are much higher levels of 2ω light; a filter with transmission 0.0321 was placed in the isolated 2ω light to avoid counter-saturation. The peak of the normalized signal is slightly more than two orders of magnitude greater than in figure 1(B). In the least-squares fit, $\chi_{\perp\parallel\parallel}$ and $\chi_{\parallel\parallel\perp}$ were held at the values determined in figures 1(A) and (B), with the only free parameter being $\chi_{\perp\perp\perp}$. The resulting fit to $R(2\omega)$ is good, with both theory and experiment showing a gradual rise to a peak at $\theta \cong 76^\circ$, followed by a rapid fall that exhibits good agreement even through the last data point at $\theta = 86^\circ$. This result provides justification for the negative sign in $\chi_{\parallel\parallel\perp}$; the best curve fit obtained with the sign of $\chi_{\parallel\parallel\perp}$ reversed shows a considerably more gradual rise for $\theta < 70^\circ$ and, at $\theta = 40^\circ$, reaches only one-half of the height of the fit in figure 1(C). Thus the sign of $\chi_{\parallel\parallel\perp}$ has been taken as negative. The value of $\chi_{\perp\perp\perp}$ obtained for the fit of figure 1(C) is 3.05×10^{-17} cm^2 statvolt^{-1} or 1.28×10^{-18} cm^2 V^{-1}. This value of $\chi_{\perp\perp\perp}$ has a modest but clear effect on the curve. For example, arbitrarily setting $\chi_{\perp\perp\perp} = 0$ produces a similar curve shape but with a 9% higher peak, thus resulting in a significantly poorer fit.

Finally, we close this section with a few comments regarding the results. We have tried using complex χ_{ijk} in the curve-fitting of figure 1(C), but the small improvements of fit and the small imaginary parts obtained do not provide sufficient justification for presenting these results. Throughout calculations, we have assumed $\epsilon(2\omega) = -9.926 + 0.537\,\mathrm{i}$ which was obtained by fitting theory to the resonant absorption anomalies of silver gratings coated at the same time as the sample discussed above. Further, we have assumed $\epsilon(\omega) = -67.03 + 2.44\,\mathrm{i}$ as did Sipe *et al* [5], who based this value on a survey of experimental measurements. The statistical error of $\chi_{\perp\parallel\parallel}$ and $\chi_{\parallel\parallel\perp}$ obtained from the least-squares fit was approximately 1%, while that of $\chi_{\perp\perp\perp}$ was 13%. However, we do not report these as the actual errors because other sources of error, such as long-term power drifts, probably produced larger effects. Second-harmonic power from a reference sample was measured at the beginning and end of each data set and corresponding corrections of a few percent were made in the data, but this procedure was probably not sufficient to fully correct for all such effects.

4. Discussion

We now relate our results to previous results. We are able to directly compare with two previous works that studied p to p harmonic generation with silver surfaces for $\lambda = 1064$ nm [17, 18]. In [17] a curve is presented similar in shape to figure 1(C), and a good comparison to their own 2-parameter model is presented. The height of the peak of the result is, however, one-half that of figure 1(C). In the second result reported [18], the curve for silver resembles figure 1(C) but there is a somewhat less steep rise to the peak of the curve. More significantly, in [18] the result is claimed to be more than 50 times higher than figure 1(C). We conclude that figure 1(C) has

similar appearance to previous results, but there is considerable disagreement on the absolute scale. There have been other measurements of this type reported elsewhere for different ω [1]–[3]; however the effects are significantly ω-dependent so that we do not discuss these further.

Another quantity that may be considered is the polarization parameter M defined by Brown and Parks [1] as, for $\theta = 45^\circ$, the ratio of $P(2\omega)$ for $(\gamma, \gamma') = (90^\circ, 0^\circ)$ to that for $(\gamma, \gamma') = (0^\circ, 0^\circ)$. This was then considered a measure of the relative importance of the bulk contribution, and may be expressed in ratios of expressions involving χ_{ijk} from equation (1). From our experimental results we obtain $M = 0.020$. Previous values have been reported as $M = 0.029$ [1] or $M = 0.066$ [2] for silver, although these results were at lower ω.

There has recently been a report of measurements of the surface nonlinear susceptibilities for sputtered silver samples [19]. The susceptibilities were determined through polarimetric second-harmonic measurements at mean fundamental wavelength 810 nm. The susceptibilities reported involve the dielectric constant $\epsilon'(\Omega)$ of an additional thin layer (as did Heinz [15]; see equations (7)–(9)) and we find it more straightforward to discuss their results for the dimensionless parameters a, b and d, for which they quote ranges of $5 \leqslant |a| \leqslant 10$, $0.27 \leqslant |b| \leqslant 0.34$ and $0.063 \leqslant |d| \leqslant 0.073$ for several silver samples. Our own values of these parameters follow from our results for $\chi_{\perp\perp\perp}$, $\chi_{\perp\parallel\parallel}$ and $\chi_{\parallel\parallel\perp}$, using equations (10)–(15) and the simplifying assumptions discussed in section 2. We thus obtain $(a, b, d) = (-0.548, -1.77, 1.07)$, where we have suppressed small ($\leqslant 0.02$) imaginary parts. Comparing the two results, it is clear that our value of a is of significantly smaller magnitude, while our b and d are considerably larger in magnitude. The reason for these differences is not clear, although the sample of [19] was prepared with a different method, the wavelength there was smaller, and the illumination spot had a 10μm width (more than two orders of magnitude smaller than our case). There is also a more subtle point: the light source of [19] produces 50 fs pulses which implies a broad spectrum of more than 40 nm width. Thus their measurement represents, in reality, sum frequency generation between all pairs of frequencies present. However, we can only contrast the experimental conditions and the actual reasons for the differences in a, b and d remain unclear.

Many other works have considered the parameters a, b and d over the years. In their hydrodynamic model, Sipe *et al* [5] have shown that $b = -1$, they have implicitly assumed that $d = 1$, and they discuss that a is of order unity, except near the plasma resonance where it can be of larger magnitude. Our experimental conditions are far from the plasma resonance, and Sipe *et al* assumed values of a between -2 and 2 for calculations they performed for $\lambda = 1064$ nm. Elsewhere, in fits to experimental data for silver coated on a glass prism with $\lambda = 1064$ nm, $a = 0.9$ has been reported [25], and in another such paper a has been reported as within range of values between -9 and 7 [26], depending on surface preparation, with b being determined as -0.97.

Other theoretical works have developed a variety of models of surface second-harmonic generation and have reported the resulting parameters. In the hydrodynamic theory of Corvi and Schaich [7], $d = 1$, $b = -1$ in many cases, and a often presents a complicated dependence on ω and ranges between -15 and 20, although it is closer to unity well below the plasma frequency. In the model of polarizable entities of Mendoza and Mochán [13], it is found that $(a, b, d) = (-29.8, -1, 1)$, where we have evaluated their expression for a using the values of $\epsilon(\omega)$ and $\epsilon(2\omega)$ employed here. However, they state that their model may have shortcomings for a conducting medium. There have been many other efforts made to calculate these dimensionless parameters for various models [8]–[12], [14], where a wide variety of numerical results have been obtained, especially for the parameter a.

We conclude that previous work does not make clear what values of a, b and d are to be expected for an evaporated silver surface under our experimental conditions. Based on the range of values quoted in previous papers, we may summarize that our result $d = 1.07$ compares well with a number of previous works, and that the result $b = -1.77$ is of somewhat larger magnitude than is commonly reported. In the case of the parameter a, our value of -0.548 is not unusual, but there has been such a wide range of values reported in both theoretical and experimental works that it is difficult to draw stronger conclusions.

5. Conclusions

We have presented experimental results for the polarization-dependence of second-harmonic generation from a silver surface. By employing photon-counting techniques and a 100 ps pulsed light source, we have been able to overcome some of the common problems of such experiments. The data are reproducible, appear to be well-isolated from stray light, and there has been no surface damage or surface plasma generation. It has thus been possible to take detailed data for the polarization-dependence, even at signal levels more than two orders of magnitude below those of the usual p to p polarization conditions.

These data hare provided a good fit with the corresponding theoretical expressions, allowing us to determine numerical values for the three unique effective surface susceptibilities. In particular, two datasets separately yield $|\chi_{\perp\parallel\parallel}|$ and $|\chi_{\parallel\parallel\perp}|$. Taking $\chi_{\perp\parallel\parallel}$ as positive, a third dataset determines the relative sign of $\chi_{\parallel\parallel\perp}$ as well as the signed numerical value of $\chi_{\perp\perp\perp}$. Other polarization conditions could also prove useful in future work, leading to interference terms between the β's of equation (1) whose effects could be varied with δ and δ', possibly improving the accuracy of the technique. However, here we have chosen a more basic approach that isolates each of β_{pp}, β_{sp} and β_{+s} in three measurements.

We have also made comparisons with previous work, although these comparisons have been largely qualitative due to the limited number of controlled experiments and the wide variety of theoretical results. It is hoped that the results presented here will prove useful and stimulate further work in this field. As was stated in section 1, a clear application of our results appears to be in rough surface harmonic generation, where existing experimental results should now be more directly comparable with recently developed theoretical formulations.

Acknowledgments

This research was supported under CICESE Internal Project 7329 and by CONACYT grant 41947F. This work was also supported by INFM, MIUR and EC grant N.RII3-CT-2003-506350. One of us (KAO'D) thanks the Fondazione Marchi for financial support.

References

[1] Brown F and Parks R E 1965 Magnetic-dipole contribution to optical harmonics in silver *Phys. Rev. Lett.* **16** 507–9

[2] Bloembergen N, Chang R K, Jha S S and Lee C H 1968 Optical second-harmonic generation in reflection from media with inversion symmetry *Phys. Rev.* **174** 813–22

[3] Wang C S and Duminski A N 1968 Second-harmonic generation of light at the boundary of alkali halides and glasses *Phys. Rev. Lett.* **20** 668–71
[4] Rudnick J and Stern E A 1972 Second-harmonic radiation from metal surfaces *Phys. Rev.* B **4** 4274–90
[5] Sipe J E, So C Y, Fukui V and Stegeman G I 1980 Analysis of second-harmonic generation at metal surfaces *Phys. Rev.* B **21** 4389–402
[6] Sipe J E and Stegeman G I 1982 Nonlinear optical response of metal surfaces *Surface Polaritons* ed V M Agranovich and D L Mills (Amsterdam: North-Holland)
[7] Corvi M and Schaich W L 1986 Hydrodynamic-model calculation of second-harmonic generation at a metal surface *Phys. Rev.* B **33** 3688–95
[8] Weber M and Liebsch A 1987 Density-functional approach to second-harmonic generation at metal surfaces *Phys. Rev.* B **35** 7411–6
[9] Liebsch A 1988 Second-harmonic generation at simple metal surfaces *Phys. Rev. Lett.* **67** 1233–6
[10] Schaich W L and Liebsch A 1988 Nonretarded hydrodynamic-model calculation of second-harmonic generation *Phys. Rev.* B **37** 6187–92
[11] Liebsch A and Schaich W L 1989 Second-harmonic generation at simple metal surfaces *Phys. Rev.* B **40** 5401–10
[12] Maytorena J A, Mochán W L and Mendoza B S 1995 Hydrodynamic model for second-harmonic generation at conductor surfaces with continuous profiles *Phys. Rev.* B **51** 2556–62
[13] Mendoza B S and Mochán W L 1996 Exactly solvable model of surface second-harmonic generation *Phys. Rev.* B **53** 4999–5006
[14] Schaich W L 2000 Calculations of second-harmonic generation for a jellium metal surface *Phys. Rev.* B **61** 10478–83
[15] Heinz T F 1982 Nonlinear optics of surfaces and adsorbates *PhD Thesis* University of California, Berkeley
[16] Mizrahi V and Sipe J R 1988 Phenomenological treatment of surface second-harmonic generation *J. Opt. Soc. Am.* B **5** 660–7
[17] Coutaz J L, Maystre D, Nevière M and Reinisch R 1987 Optical second-harmonic generation from silver at 1.064-μm pump wavelength *J. Appl. Phys.* **62** 1529–31
[18] Akhmediev N V, Mel'nikov I V and Robur L J 1994 Second-harmonic generation by a reflecting metal surface *Laser Phys.* **4** 1194–7
[19] Krause D, Teplin C W and Rogers C T 2004 Optical surface second harmonic measurements of isotropic thin-film metals: gold, silver, copper, aluminum and tantalum *Phys. Rev.* B **96** 3626–34
[20] Shen Y R 2000 IEEE journal on selected topics in quantum electronics *Phys. Rev.* B **6** 1375–9
[21] Leskova T A, Maradudin A A and Méndez E R 2002 Multiple-scattering phenomena in the second-harmonic generation of light reflected from and transmitted through randomly rough metal surfaces *Optical Properties of Nanostructured Random Media* ed V M Shalaev (Berlin: Springer) and references therein
[22] Gayot-Sionnest P and Shen Y R 1988 Bulk contribution in surface second-harmonic generation *Phys. Rev.* B **38** 7985–9
[23] Gayot-Sionnest P, Chen W and Shen Y R 1986 General considerations on optical second-harmonic generation from surfaces and interfaces *Phys. Rev.* B **33** 8254–63
[24] Jerphagnon J and Kurtz S K 1970 Maker fringes: a detailed comparison of theory and experiment for isotropic and uniaxial crystals *J. Appl. Phys.* **41** 1667–81
[25] Quail J C and Simon H J 1983 Second-harmonic generation from silver and aluminum films in total internal reflection *Phys. Rev.* B **31** 4900–5
[26] Jiang H B, Li L, Wang W C, Zheng J B, Zhang Z M and Chen Z 1991 Reflected second-harmonic generation at a silver surface *Phys. Rev.* B **44** 1220–4